Studies of Electronic Coupling and Mixed Valency in Metal−Metal Quadruply Bonded Complexes Linked by Dicarboxylate and Closely Related Ligands

MALCOLM H. CHISHOLM* AND NATHAN J. PATMORE
Department of Chemistry, The Ohio State University, 100 West 18th Avenue, Columbus, Ohio 43210-1185

Received April 10, 2006

ABSTRACT

Complexes of the form $[(^tBuCO_2)_3M_2]_2(\mu\text{-}O_2C{-}X{-}CO_2)$, where M is Mo or W and X is a π conjugated organic group, are ideally suited for studies of electronic coupling between the two redox centers via M_2 δ-bridge π conjugation. The complexes have intense metal-to-bridge charge-transfer transitions in the visible or near-IR region of the spectrum and exhibit thermo-, solvato- and electrochromic behavior. Chemical oxidation results in the formation of mixed-valence species that are particularly well-suited for the study of the class II/III border. The extent of electronic coupling is determined by a variety of spectroscopic techniques and, in particular, by EPR and electronic absorption spectroscopy. The latter provides a direct measure of the electronic coupling parameter H_{ab} in pairs (Mo and W) of otherwise identical complexes. Similarly, the substitution within the bridge of the CO_2 group by COS or RNCO allows an evaluation of the mechanism of the electronic coupling in closely related complexes. Electronic structure calculations employing density functional theory complement frontier molecular orbital theory in the interpretation of the physicochemical properties of these complexes.

Introduction

Electron transfer and electron delocalization are ubiquitous in chemistry, physics, and biology, and studies of two redox active centers connected by a bridge provide an ideal template upon which to extract intricate mechanistic details concerning the factors controlling these processes. It is now just 40 years since the influential publication by Robin and Day wherein the nomenclature of classes I, II, and III was introduced to describe valence trapped, strongly coupled, and fully delocalized mixed valence systems, respectively.[1] In the same year, Hush published his pioneering work on the interpretation of the phenomenon of intervalence charge transfer absorptions,[2] and soon after, Creutz and Taube reported their initial studies of the ions $[(NH_3)_5Ru(\mu\text{-pz})Ru(NH_3)_5]^{4+/5+/6+}$ where pz = 1,4-pyrazine.[3] There ensued a flood of interest in these matters,[4−7] which continues to this day with a special emphasis on the class II/III border,[8,9] vibronic−electronic coupling,[10,11] and the discovery of mixed valence isomers.[12,13] Much of the work has centered on d^5−d^6 metal ions in pseudo-octahedral environments.[14] In this Account, we review some of our studies of a series of complexes of the formula $[(^tBuCO_2)_3M_2]_2(\mu\text{-bridge})$ where the quadruply bonded metal ions are either molybdenum or tungsten and the bridge is a dicarboxylate or a closely related bridge wherein one oxygen atom of the carboxylate function is replaced by a S atom or a NR group.

These complexes contain metal−metal (MM) quadruple bonds of configuration $\sigma^2\pi^4\delta^2$ and have many attractive features for the study of electronic coupling and mixed valence:

(1) Largely as a result of work from the Cotton group, there is a vast structural database for M_2^{4+}, M_2^{5+}, and M_2^{6+} complexes of molybdenum and tungsten having the paddle-wheel structural motif.[15] Thus, single-crystal X-ray crystallography can be extremely useful in determining the location of charge in mixed valence systems.[16,17]

(2) Molybdenum and tungsten have effectively the same size, so for compounds having the same bridging group, solvation and reorganizational effects are very similar. Differences in electronic coupling arise from the differences in valence orbital energies and in the radial extension and overlap of the d orbitals.

(3) The electronic structures of these paddle-wheel complexes are understood as a result of extensive computational studies, and these correlate well with a good spectroscopic databank.[18,19]

(4) Both molybdenum and tungsten exist in a variety of naturally occurring isotopes, the majority of which have no nuclear spin. However, some do, and the presence of ^{183}W, $I = {}^1/_2$ (14.3% natural abundance), and the two molybdenum isotopes, ^{95}Mo and ^{97}Mo, $I = {}^5/_2$ (25.4% combined natural abundance), make EPR spectroscopy a most

Malcolm Chisholm was born in India in 1945 to Scottish parents and educated in England, B.Sc. 1966, Ph.D. 1969 at London University, Queen Mary College. After a postdoctoral appointment at the University of Western Ontario, he was appointed to the faculty at Princeton University and from there moved to Indiana University and the Ohio State University where he is currently a Distinguished Professor of Mathematical and Physical Sciences. His research interests embrace various aspects of inorganic, organometallic, and materials chemistry. He has served as an associate editor for *Chemical Communications*, *Dalton Transactions*, and *Polyhedron*. He is a member of the National Academy of Sciences (U.S.A.), the German Academy-Leopoldina, and the Royal Societies of London and Edinburgh.

Nathan Patmore was born in England in 1977 and obtained both his B.Sc. (Hons) degree (1999) and Ph.D (2002) at the University of Bath, U.K. His postgraduate research was performed under the supervision of Dr. Andrew Weller, based on the incorporation of weakly coordinating anions into organometallic fragments. He joined the group of Prof. Malcolm Chisholm at the Ohio State University in 2002, focusing on the study of electronically coupled quadruply bonded M_2 compounds. In 2005, he took up an independent position as a Ramsay Memorial Research Fellow at the University of Sheffield and in 2006 was awarded a Royal Society University Research Fellowship. His current research interests are in the use of diruthenium paddle-wheel compounds to generate useful electronic and magnetic materials.

* To whom correspondence should be addressed. E-mail: chisholm@chemistry.ohio-state.edu.

10.1021/ar068100i CCC: $37.00
Published on Web 10/12/2006

valuable probe. Upon single-electron oxidation of the complex, EPR spectroscopy can establish unequivocally whether the metal center has been oxidized and, if so, the degree of electron delocalization of the unpaired electron.[20,21]

Synthesis

A general synthetic procedure leading to the dicarboxylate-bridged compounds is shown in eq 1.[22]

$$2M_2(O_2C^tBu)_4 + HO_2C{-}X{-}CO_2H \xrightarrow[25\ ^\circ C,\ >1\ day]{\text{toulene}} [(^tBuCO_2)_3M_2]_2(\mu\text{-}O_2C{-}X{-}CO_2) + 2\,^tBuCO_2H \quad (1)$$

Equation 1 is actually an equilibrium reaction, but the desired dicarboxylate-bridged complex precipitates from toluene as a fine microcrystalline precipitate driving the reaction to completion. The reaction time is typically longer than 1 day because the dicarboxylic acids are often very sparingly soluble in toluene. The microcrystalline powders are collected by either filtration or centrifugation and are washed first with toluene and hexanes to remove any unreacted $M_2(O_2C^tBu)_4$ and then with ethanol to remove any unreacted dicarboxylic acid. Upon drying under vacuum, the dicarboxylate-linked M_4-containing complexes are obtained as analytically pure, air-sensitive, intensely colored materials. Their colors arise from metal to bridge charge transfer absorptions (*vide infra*). The use of dicarboxylate bridges such as oxalate and terephthalate aligns the M_2 axes in a parallel manner at a specific M_2 to M_2 distance, while the use of anthracene-1,8-dicarboxylate aligns the M_4 unit in a chain with a very short M_2-to-M_2 distance, ca. 3 Å. These orientations are diagrammatically depicted by **A** and **B** in Scheme 1, along with some representative dianionic bridges.

An alternative synthetic procedure that works well for molybdenum involves the metathetic reaction between $[Mo_2(O_2C^tBu)_3(CH_3CN)_2]^+[PF_6]^-$, and the salt of a dicarboxylic acid or related bridging dianion in a solvent such as acetonitrile or dichloromethane.[23]

Scheme 1

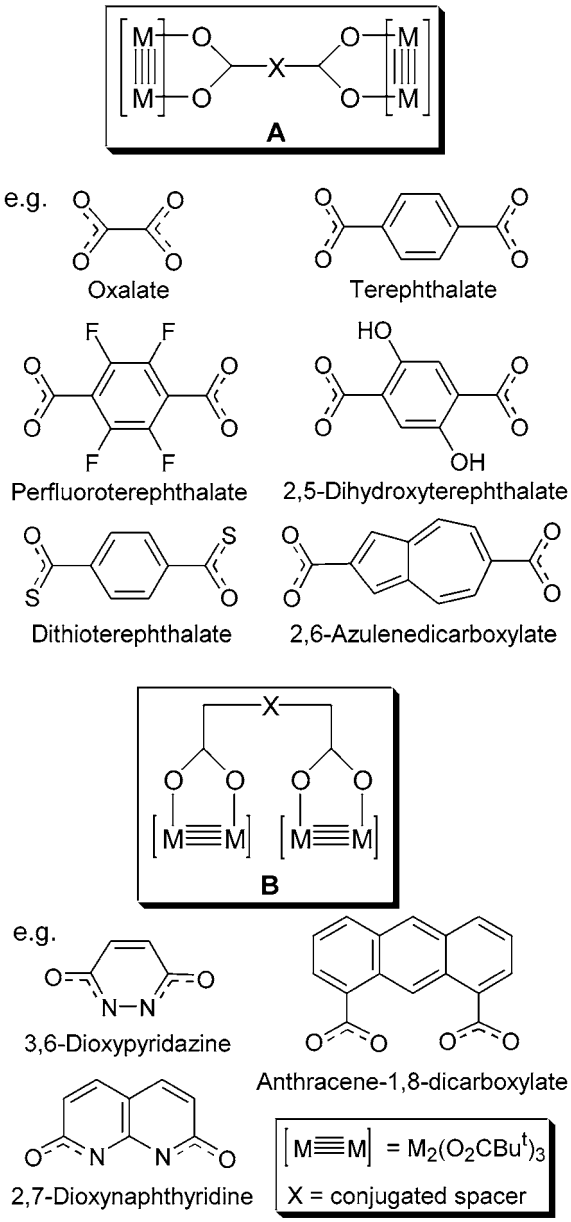

The Origin of Electronic Coupling: Electronic Structures

The origin of the electronic coupling of the two M_2 centers is best exemplified by the oxalate bridge ($O_2CCO_2^{2-}$). All other $O_2C{-}X{-}CO_2$ bridges are only modified by the additional $CO_2{-}X$ π orbital interactions. The CO_2 units act as alligator clips in providing both the means of covalently linking the two M_2 units in a σ-bonded manner and, via M_2 δ to CO_2 π conjugation, the electrical conduit for delocalization. The in- and out-of-phase M_2 δ orbitals interact with the planar oxalate π orbitals, as shown in Scheme 2. Of these two orbital interactions, the in-phase M_2 δ combination is the most important and provides stabilization for the planar bridge conformation by means of back-bonding from the metal. The M_2 $\delta{-}$bridge LUMO interaction is stronger for M = W (relative to M = Mo) because the W_2 δ orbitals are higher in energy by roughly 0.5 eV. The M_2 δ out-of-phase combination interacts with a filled oxalate π MO and as such raises the energy of this M_2 δ combination. The oxygen-based π MO

Scheme 2

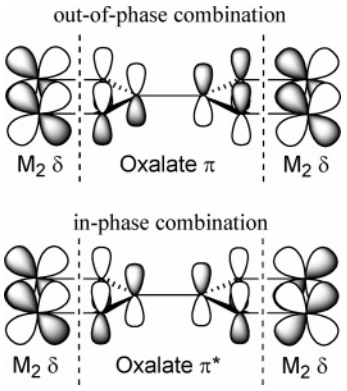

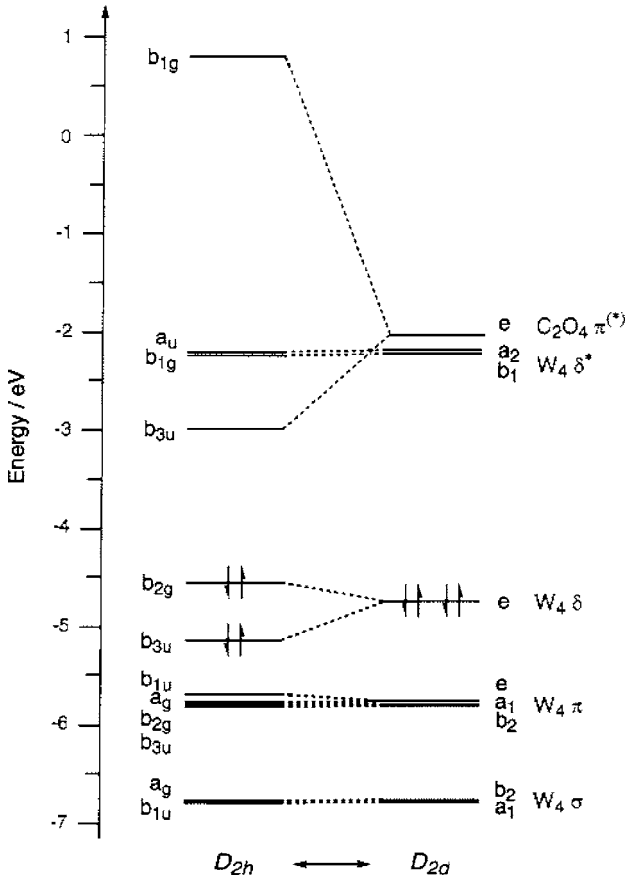

FIGURE 1. Walsh diagram relating the calculated frontier MO energies for the D_{2h} planar and D_{2d} twisted geometries of $[(formate)_3W_2]_2(\mu\text{-}O_2CCO_2)$. Reproduced with permission from ref 24. Copyright 2002 American Chemical Society.

is notably much lower in energy than the M_2 δ orbitals and thus causes a much less significant effect. However, this interaction becomes more important upon replacing an oxygen atom by sulfur or a NR group (*vide infra*). From the orbital interactions shown in Scheme 2, it is apparent that electronic communication is maximum for the planar bridge (D_{2h} symmetry) and a minimum for the fully twisted D_{2d} structure. These positions thus represent on and off in what may be viewed as a molecular rheostat with variation of the O_2C-CO_2 dihedral angle.

Electronic structure calculations employing density functional theory on model compounds where formate ligands are substituted for pivalates provide a much more quantitative interpretation of the electronic structure of these types of compounds, and a Walsh frontier orbital energy diagram for the $[(formate)_3W_2]_2(\mu\text{-}O_2CCO_2)$ model complex in the planar and twisted forms is shown in Figure 1.[24]

The HOMO−LUMO electronic transition represents a metal to bridge charge transfer (MLCT) and is fully allowed. As can be seen from Figure 1, the energy gap of the HOMO−LUMO orbitals is very sensitive to the O_2C-CO_2 dihedral angle. Since the free oxalate dianion favors a D_{2d} geometry, the energy barrier to rotation is relatively small: $\Delta G_{rot} \approx 9$ kcal mol^{-1} for M = W and

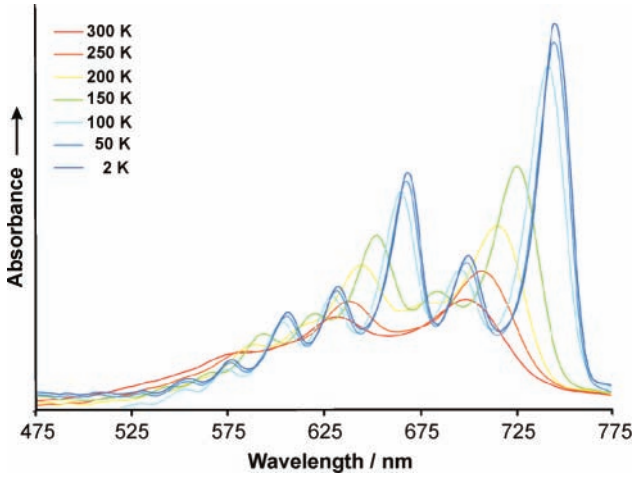

FIGURE 2. Electronic absorption spectra of $[(^tBuCO_2)_3W_2]_2(\mu\text{-}O_2CCO_2)$ at 2, 50, 100, 150, 200, 250, and 300 K in 2-methyltetrahydrofuran solution. Reproduced with permission from ref 24. Copyright 2002 American Chemical Society.

$\sim$5 kcal mol^{-1} for M = Mo from electronic structure calculations.[24] Consequently, the oxalate- and related terephthalate-bridged complexes show thermochromism in solutions and frozen glasses. The spectra recorded for the tungsten oxalate-bridged complex in 2-methyltetrahydrofuran from room temperature to 2 K are shown in Figure 2.

These complexes show intense resonance Raman enhanced bands associated with ν(MM) and bridge stretching modes when the wavelength of excitation falls within the envelope of the HOMO−LUMO, the metal to bridge transition.[17,25]

As conjugation increases along the bridge, the HOMO−LUMO gap decreases and the metal to bridge charge transfer moves into the near-IR. From transient absorption spectroscopy, the photoexcited states have been found to be long-lived ($\sim$50 μs), and the ^{1}MLCT states have been observed directly.[26]

Finally, it is worth noting that these complexes are also solvatochromic, and in certain solvents, they tend to associate in solution via intermolecular $M_2\cdots O$ bridges. This has a pronounced effect on the nature of the absorption spectra just as does the $\pi-\pi$ stacking of aromatics in solution.[27]

Electrochemical Studies

The linked dinuclear complexes when examined by cyclic voltammetry (CV) and differential pulse voltammetry (DPV) typically show reduction waves corresponding to bridge reductions, and two waves resulting from oxidation of the M_2 units. In general, the first oxidation wave is reversible and the second quasi-reversible. The separation of the first and second waves, $\Delta E_{1/2}$ (measured in millivolts), can be used to determine a comproportionation constant relating the stability of the singly oxidized complex in relation to an equilibrium with the neutral and

Table 1. Summary of Electrochemical Data for $[(^tBuCO_2)_3M_2]_2(\mu$-bridge) (M = Mo, W) Compounds[a]

bridge	$E_{1/2}(1)$, V	$E_{1/2}(2)$, V	$\Delta E_{1/2}$, mV	K_c	ref
	M = Mo				
oxalate	−0.03	0.25	280	5.4×10^4	22
terephthalate[b]	−0.10			~4	31
perfluoroterephthalate	0.10		65	1.3×10^1	22
2,5-dihydroxyterephthalate	0.00	0.08	79	2.1×10^1	32
2,6-azulenedicarboxylate	−0.09	0.02	112	7.8×10^1	34
dithioterephthalate	0.00	0.18	184	1.3×10^3	38
anthracene-1,8-dicarboxylate[c]	0.06				33
3,6-dioxypyridazine	−0.15	0.28	280	5.4×10^4	23
2,7-dioxynaphthyridine	−0.07	0.32	389	3.8×10^6	22
	M = W				
oxalate	−1.26	−0.54	717	1.3×10^{12}	22
terephthalate	−0.34	−0.18	160	5.1×10^2	32
perfluoroterephthalate	−0.66	−0.37	285	6.6×10^4	22
2,5-dihydroxyterephthalate	−0.72	−0.52	202	2.6×10^3	32
2,6-azulenedicarboxylate	−0.91	−0.44	468	8.2×10^7	34
dithioterephthalate	−0.78	−0.26	518	5.7×10^8	38
anthracene-1,8-dicarboxylate	−0.66	−0.51	156	4.3×10^2	33
3,6-dioxypyridazine	−0.91	−0.28	630	4.5×10^{10}	17

[a] Voltammograms were recorded in $^nBu_4NPF_6$/THF solutions and referenced to the $FeCp_2^{0/+}$ couple. [b] Single redox process observed corresponding to two overlapping one-electron oxidation processes. [c] Second oxidation potential obscured by anthracene oxidation processes. Potentials converted to the $FeCp_2^{0/+}$ reference.

doubly oxidized complexes:[28]

$$[M_2{-}bridge{-}M_2] + [M_2{-}bridge{-}M_2]^{2+} \overset{K_c}{\rightleftharpoons} 2[M_2{-}bridge{-}M_2]^{+} \quad (2)$$

$$K_c = \left[\exp\frac{(E^1_{1/2} - E^2_{1/2})F}{RT}\right] = \exp\left(\frac{\Delta E_{1/2}}{25.69}\right) \quad \text{at 298 K, } \Delta E_{1/2} \text{ in mV} \quad (3)$$

It is important to recognize that K_c is a thermodynamic parameter and as such does not correlate directly with electronic coupling through M_2 δ−bridge π bonding. Particularly important are such factors as solvent, counteranion, and number of redox centers,[17,29,30] thus any comparison of $\Delta E_{1/2}$ and K_c values must relate to otherwise identical systems obtained under similar experimental conditions. This having been stated, we summarize some pertinent electrochemical data in Table 1 for selected bridged M_4-containing species. All the data presented were obtained from tetrahydrofuran solutions with $N^nBu_4PF_6$ as electrolyte. The importance of maintaining the counteranion constant is seen in the following. The terephthalate-bridged Mo_4-containing complex has a single somewhat broad CV wave and DPV curve with PF_6^- as the counteranion, but with $B(C_6H_3{-}\{CF_3\}_2)_4^-$ two well-resolved waves are seen leading to K_c values of ~4 and 324, respectively.[31]

The data in Table 1 reveal some interesting trends, and most notably, (i) the K_c values are always greater for M = W than for M = Mo and (ii) K_c decreases with increasing distance. For a series of substituted terephthalate-bridged tungsten complexes, we also observed that K_c correlates with energy of the HOMO−LUMO transition.[32] Since the HOMO is the out-of-phase combination of the M_2 δ orbitals, we can see that K_c also correlates with the degree of the in-phase M_2 δ interaction with the bridge π^* LUMO, and the energy difference between the HOMO and HOMO − 1.

From an inspection of Table 1, it is also apparent that K_c values do not correlate with M_2 to M_2 distance in compounds that have M_4 chains (Scheme 1, structure **B**). Despite bringing the M_2 centers within ~3 Å, the communication is very poor for the anthracene-1,8-dicarboxylate-bridged compounds[33] but much better for the stereo correspondent 2,7-dioxynaphthyridine bridge[22] demonstrating the importance of the bridge in mediating electronic coupling. It is also interesting to note that the substitution of S or RN within the CO_2 linker has an apparent greater effect for molybdenum complexes than for tungsten, and we shall return to this point later.

Finally, it is worth noting that while a large value of K_c (>10^6) is surely indicative of strong coupling, it is not possible to formulate a distinction between class II and class III behavior based on electrochemical data alone.

EPR Data and Electron Delocalization

Only in rare cases has oxidation with $AgPF_6$ or Cp_2FePF_6 led to isolable stable radical cationic M_4-containing complexes with carboxylate ancillary ligands. In most instances, the oxidized species are subject to ligand scrambling and redox disproportionation. However, it has been possible to examine the EPR spectra of freshly prepared samples and evaluate the nature of the electron delocalization. In order to emphasize the importance of this approach, it is informative to appreciate the EPR spectra of the radical cations $Mo_2(O_2C^tBu)_4^+$, $MoW(O_2C^tBu)_4^+$, and $W_2(O_2C^tBu)_4^+$, which are shown in Figure 3. Each solution spectrum consists of a central signal at $g \approx 1.8{-}1.9$ due to a M_2 δ based electron where the metal isotopes have $I = 0$. The satellite spectra arise from coupling to ^{95,97}Mo or ^{183}W, which have $I = {}^5/_2$ and ${}^1/_2$, respectively. For the Mo_2^{5+} center, the hyperfine coupling constant $A_0 = 27$ G and for W_2^{5+} $A_0 = 51$ G. The spectrum of the mixed metal-containing complex with the single electron in the MoW δ orbital shows coupling to both ^{95,97}Mo ($A_0 = 44$ G) and ^{183}W ($A_0 = 31$ G) consistent with the polarization of the MoW δ orbital where the odd electron has greater Mo d orbital character than in the Mo_2^{5+} ion. Specifically, modeling indicates 71% Mo and 29% W atomic orbital contributions.[21]

The observed and calculated EPR spectra for the oxalate- and terephthalate-bridged Mo_4-containing radical cations are shown in Figure 4. For the oxalate complex ion, $A_0 = 15$ G corresponds to the single electron being delocalized over all four Mo atoms whereas for the terephthalate-bridged complex ion $A_0 = 27$ G and the complex is valence trapped on the EPR time scale with one Mo_2^{5+} and one Mo_2^{4+} center.[20]

For tungsten, electron delocalization has been seen for terephthalate-bridged species[32] and in the case of the 2,6-azulene dicarboxylate-bridged complex where the two W_2 centers are separated by ~14 Å, the satellite spectrum

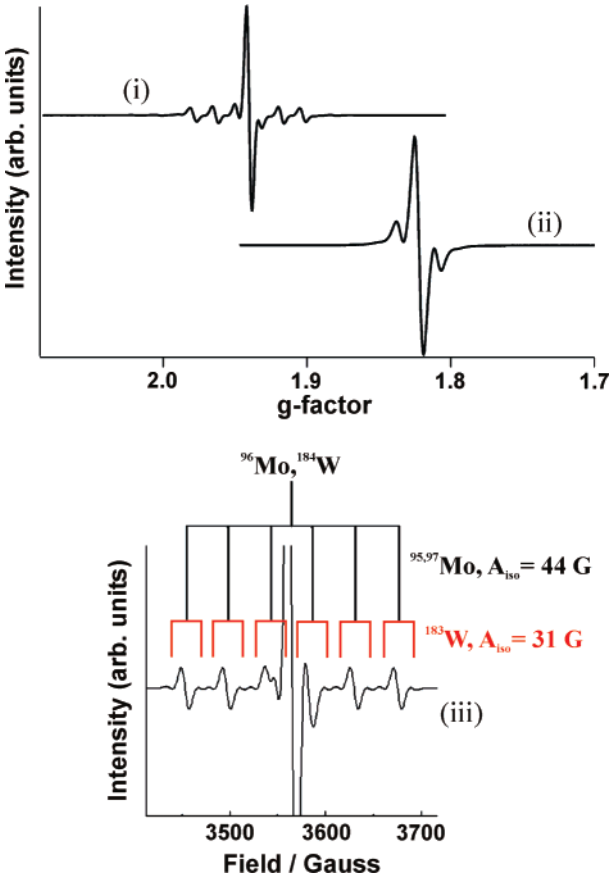

FIGURE 3. Solution EPR spectra of $Mo_2(O_2C^tBu)_4^+PF_6^-$ (i) and $W_2(O_2C^tBu)_4^+PF_6^-$ (ii) in dichloromethane at 210 K (top), and $MoW(O_2C^tBu)_4^+PF_6^-$ (iii) in THF at 225 K (bottom). Reproduced with permission from ref 21. Copyright 2005 American Chemical Society.

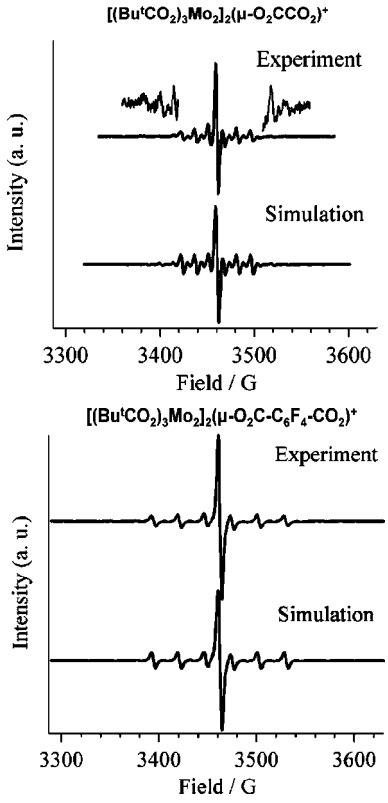

FIGURE 4. Solution EPR spectra of $[(^tBuCO_2)_3Mo_2](\mu\text{-}O_2CCO_2)^+PF_6^-$ ($g_{iso} = 1.937$, $A_{iso} = 14.8$ G) and $[(^tBuCO_2)_3Mo_2]_2(\mu\text{-}O_2C{-}C_6F_4{-}CO_2)^+PF_6^-$ ($g_{iso} = 1.942$, $A_{iso} = 27.2$ G) recorded in 2:1 THF/CH_2Cl_2 mixtures. Spectral simulations were performed using Bruker SimFonia. Reproduced with permission from ref 20. Copyright 2002 Royal Society of Chemistry.

reveals coupling to two inequivalent W_2 centers, $A_0 = 20$ and 41 G, consistent with electron polarization in the singly occupied highest molecular orbital.[34] This arises because azulene is a polar molecule having a dipole moment of ~1 D. The appearance of two hyperfine coupling constants indicates that the compound is not a rare example of a "mixed-valence isomer"[12] and shows the potential for EPR spectroscopy in characterizing such systems.

In the radical cation of the 3,6-dioxypyridazine-bridged Mo_4 complex, two sets of A_0 values (12.4 and 15.6 G) were also observed.[35] Each Mo atom within each Mo_2 unit is bonded to either oxygen or nitrogen as shown below in structure **C**.

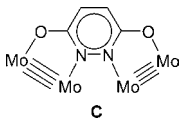

C

The A_0 values indicate that the single electron is delocalized over all four Mo atoms, but the Mo_2 units are polarized.

Electron delocalization on the EPR time scale indicates that if the system is not fully delocalized then electron transfer must be quicker than $\sim 10^9$ s^{-1}. A more quantitative measure of electronic coupling and delocalization on a faster time scale is obtained from electronic and vibrational spectroscopies.

Intervalence Charge Transfer and Charge Resonance Bands

As indicated in the introduction, the radical cations of these bridged M_2 complexes are well suited for studies of mixed valency since only one metal orbital on each M_2 center is involved. Before we discuss the observed spectra in the near IR, it is worthwhile reviewing what is expected based on current two-state classical Marcus−Hush theory.[2,9]

In Figure 5, we show potential energy curves for a mixed valence class II compound (panel I), a compound at the Class II/III border where $\Delta G^{\ddagger}$ (thermal) = 0 (panel II) and a fully delocalized, strongly coupled compound (panel III). The class II situation corresponds to that described by Hush where a relatively broad and Gaussian-shaped absorption profile is expected. The vertical transition corresponds to $\bar{\nu}_{max} = \lambda$, where λ is the reorganizational energy, and the electronic coupling parameter H_{ab} can be determined experimentally using eq 4:

$$H_{ab} = (0.0206/d)(\bar{\nu}_{max}\Delta\bar{\nu}_{1/2}\epsilon_{max})^{1/2} \qquad (4)$$

where d is the electron-transfer distance (Å), $\bar{\nu}_{max}$ is the energy of the intervalence band (cm^{-1}) at maximum

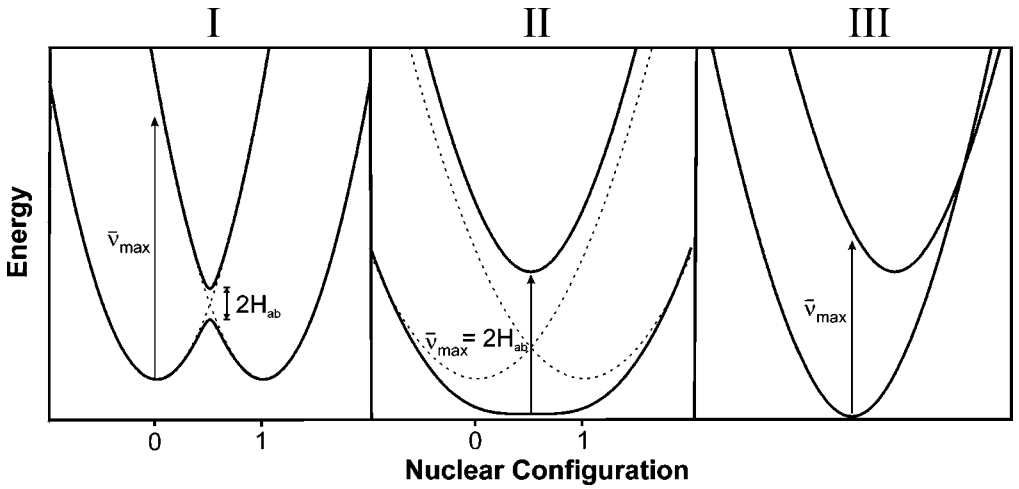

FIGURE 5. Potential energy curves for symmetrically bridged dinuclear systems for (I) a weakly coupled species ($H_{ab} = \lambda/18$), (II) a compound on the class II/III borderline ($H_{ab} = \lambda/2$), and (III) a molecular absorption. The dotted lines represent the corresponding diabatic (class I) curves.

extinction coefficient, $\Delta\bar{\nu}_{1/2}$ is the peak width at half peak height (cm^{-1}), and ϵ_{max} is the peak intensity (M^{-1} cm^{-1}). As the electronic coupling increases, the thermal barrier to electron transfer goes to zero and the ground potential surface has a "flat well", as shown in Figure 5, panel II. In this situation, the low-energy transition is predicted to have a distinctly non-Gaussian shape, showing a very sharp onset of absorption at the low-energy side followed by a more Gaussian shape to higher energy. In practice, photoexcitation from vibronically excited states and solvent broadening lead to a rounding of the low-energy cutoff. For this type of class III system, the mixing term H_{ab} is simply one-half of the energy of the electronic transition.

With further electronic coupling the ground-state well sharpens and deepens and the excited-state energy minimum and ground-state minimum move apart on the reaction coordinate axes. This is because the mixed valence ion is behaving as a molecular species and the electronic transition, which is best defined as a "charge resonance" transition, involves the promotion of an electron from a bonding molecular orbital to an antibonding molecular orbital. Schematically this is shown in the simplified MO diagram given in Figure 6 for a typical $[(^tBuCO_2)_3M_2]_2(\mu\text{-}O_2C{-}X{-}CO_2)^+$ system. Interaction of a metal dπ orbital combination with the bridge π^* orbital leads to metal−bridge bonding while the filled−filled metal d_π−bridge π orbital interaction leads to a metal−bridge antibonding orbital. The LMCT highlighted in Figure 6 as a dotted line would be forbidden for the oxalate-bridged complex under rigorous D_{2h} symmetry and would be expected to be in the UV/vis region because the oxalate π orbital is ~7.5 eV below the M_2 δ orbitals.[36] As the electronic coupling increases within the class III regime, we will expect a more Gaussian-shaped absorption curve and that the absorption maximum will move to higher energy.

Ligand field asymmetry and spin−orbit coupling in mixed-valence $[M^{III}{-}bridge{-}M^{II}]^{n+}$ (M = Fe, Ru, Os) systems lead to a splitting of the t_{2g} orbitals on each metal

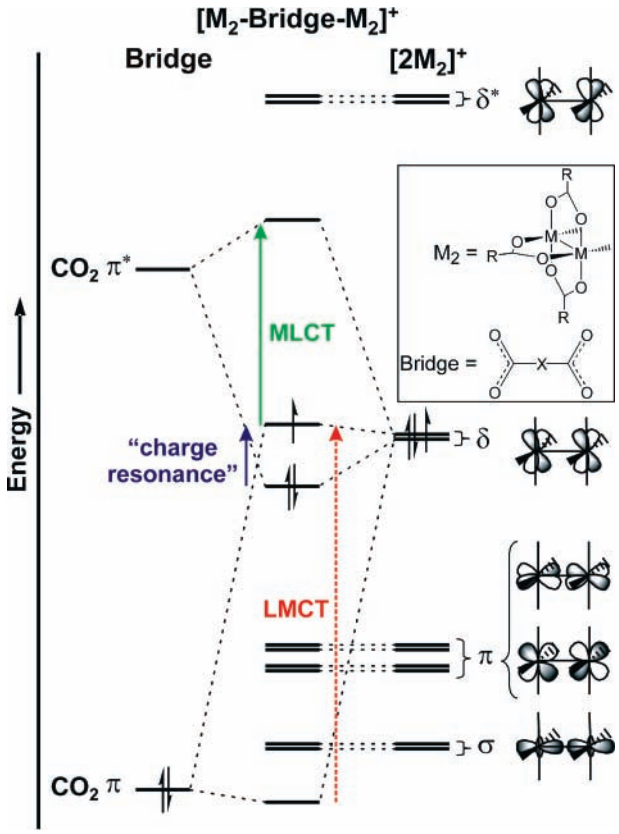

FIGURE 6. Qualitative MO diagram showing the formation of a strongly coupled $[M_2{-}bridge{-}M_2]^+$ species from $\{M_2(O_2C^tBu)_3\}$ and $\{O_2C{-}X{-}CO_2\}$ fragments. Salient electronic transitions have been highlighted.

into three dπ levels (called Kramer's doublets), which in most instances gives rise to a number of intervalence charge transfer (IVCT) and interconfigurational (IC) transitions that can complicate assignment.[14] As shown in Figure 6, the nearest metal-based orbitals to the M_2 δ combinations in $[M_2{-}bridge{-}M_2]^+$ species are the M_2 π-orbitals that are separated by ~1.2 eV from the M_2 δ combinations. This means there are no extra IVCT or IC transitions to complicate the assignment and analysis of

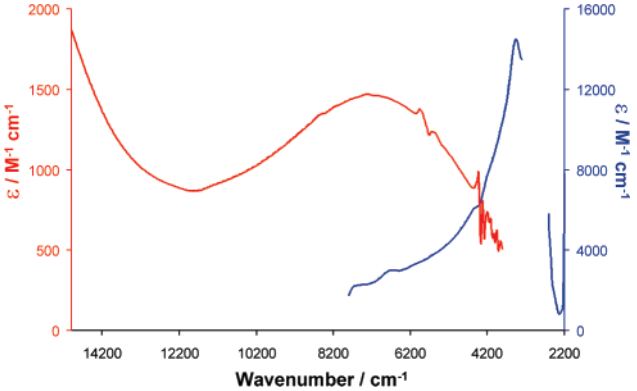

FIGURE 7. NIR electronic absorption spectra of $[(^tBuCO_2)_3M_2]_2(\mu$-2,5-dihydroxyterephthalate)$^+PF_6^-$ [M = Mo (red) and W (blue)] recorded in THF at room temperature. The gap between 2610 and 3280 cm^{-1} for $[(^tBuCO_2)_3W_2]_2(\mu$-2,5-dihydroxyterephthalate)$^+PF_6^-$ corresponds to a THF solvent absorption. Reproduced with permission from ref 32. Copyright 2005 American Chemical Society.

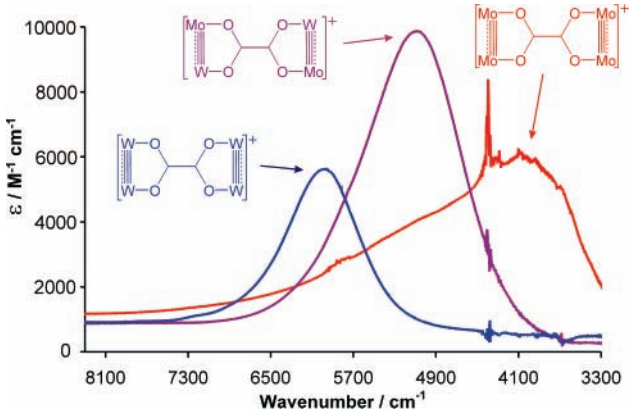

FIGURE 8. NIR electronic absorption spectra of $[(^tBuCO_2)_3M_2]_2(\mu$-$O_2CCO_2)^+PF_6^-$ [M_2 = Mo_2 (red), MoW (purple) and W_2 (blue)] recorded in THF solutions at room temperature. The spectral feature at 4400 cm^{-1} corresponds to a sample cell glass absorption.

the IVCT absorption, providing some advantage over the extensively studied t_{2g}^6−bridge−t_{2g}^5 systems.

With these considerations in mind, it is worth examining the features of some closely related complexes, and we show in Figure 7 the near-IR absorptions of the Mo_4- and W_4-containing radical cations having the 2,5-$(OH)_2$−1,4$(CO_2)_2$−C_6H_2 bridge.[32] The molybdenum complex has a broad electronic transition centered at 7200 cm^{-1}. This is typical of a class II compound, and on the basis of Hush theory, we can estimate that H_{ab} = 446 cm^{-1}. In contrast, the tungsten complex shows a much lower energy absorption of much narrower width. This is characteristic of a class III transition where H_{ab} = 1715 cm^{-1}.

Another informative series of spectra are presented in Figure 8 for the oxalate-bridged radical cations of Mo_4-, $(MoW)_2$-, and W_4-containing species.[20,36,37] Of particular note here is the progression to lower energy of the absorption maximum within the series and also the marked asymmetry of the absorption associated with the Mo_4 complex. Indeed, the features of the Mo_4-containing ion are as predicted for an ion that is close to the class II/III border (vide infra). It is, however, based on its bandwidth to the high-energy side, still reasonable to classify this ion as a class III ion, with the single electron fully delocalized over all four Mo atoms. The narrower, more Gaussian-shaped profile and shift to higher energy of the other ions are consistent with the enhanced electronic coupling of the tungsten-containing complexes.

In Table 2, we summarize some data obtained from the electronic absorption spectra of the radical cations of these linked M_2 quadruply bonded complexes which, in addition to the charge resonance band, show MLCT bands at higher energy. We see that the electronic coupling is always greater for tungsten than for molybdenum and that H_{ab} decreases with increasing distance. It is also apparent from all of the aforementioned that the dominant mechanism of electronic coupling is via the LUMO of the bridge. This is really quite interesting because in many bridges, such as the dicarboxylates of 9,10-anthracene, 2,5-thienyl, and 2,6-azulene, the HOMO of the bridge is much closer in energy to the M_2 δ orbital energy than is the M_2 δ to the bridge LUMO. Thus the carboxylate unit acts as a gate in determining the relative importance of "electron

Table 2. Summary of the NIR Absorptions Observed for Selected $[(^tBuCO_2)_3M_2]_2(\mu$-bridge$)^+PF_6^-$ (M = Mo, W) Compounds[a]

bridge	$\bar{\nu}_{max}$, cm^{-1}	$\Delta\bar{\nu}_{1/2}$(obsd)[b], cm^{-1}	$\Delta\bar{\nu}_{1/2}$(calcd)[c], cm^{-1}	ϵ_{max}, M^{-1} cm^{-1}	H_{ab}, cm^{-1}	class[d]	ref
			M = Mo				
oxalate	4000	2800	3040	6000	2000	III	20
2,5-dihydroxyterephthalate[e]	7200	5720	4078	1470	446	II	32
2,6-azulenedicarboxylate	6250	4800	3800	2070	380	II	34
			M = W				
oxalate	5960	940	3710	5620	2980	III	20
terephthalate	3220	2220	2727	18000	1610	III	32
perfluoroterephthalate	3570	582	2872	9600	1785	III	32
2,5-dihydroxyterephthalate	3430	1270	2815	14400	1715	III	32
2,6-azulenedicarboxylate	3080	750	2660	4550	1540	III	34
dithioterephthalate	4325	668	3161	8170	2163	III	38
3,6-dioxypyridazine	3775	1320	2950	5000	1888	III	17

[a] Spectra were acquired in THF solutions at room temperature. [b] Bandwidth determined from the high-energy side of the band for nonsymmetrical absorptions to avoid low-energy cutoff effects. [c] Calculated using $\Delta\bar{\nu}_{1/2} = (2310\bar{\nu}_{max})^{1/2}$. [d] Based on the observations that for a class III system $\Delta\bar{\nu}_{1/2}$(calcd) > $\Delta\bar{\nu}_{1/2}$(obsd) and the absorption intensity is typically >5000 M^{-1} cm^{-1}. [e] Class II system hence H_{ab} calculated using eq 4, with d approximated using the calculated $M_2\cdots M_2$ separation in the optimized geometry obtained from gas-phase DFT calculations.

transfer"/"hole transfer" in the coupling mechanism. With this in mind, it is useful to examine the influence of oxygen atom substitution within the CO_2 moiety of the bridge.

Substitution of O by S and NR in the CO_2 Linker

The substitution of O by S has been achieved using the dithioterephthalate bridge.[38] It shows a dramatic enhancement of electronic coupling in comparison to its closely related terephthalate analogue as indicated by both the electrochemical data (see Table 1) and the increase in energy of the charge resonance band for the tungsten complexes (Table 2). The enhanced electronic coupling arises from a lowering of the COS π^* orbital and a raising of the filled COS π orbital.

The substitution of PhN for O has been achieved by Cotton et al. in formamidinate-supported molybdenum complexes and found to lead to two isomers.[39] Unfortunately, a direct comparison with oxalate is not possible. In one isomer, the PhN(O)CC(O)NPh linker is akin to a twisted oxalate geometry, and in the other, there is a planer bridge with Mo_2OCCN six-membered rings. The latter produced a shorter Mo_2 to Mo_2 distance, and the electrochemical data indicate strong electronic coupling. In the former twisted geometry, the Mo_2 δ−bridge π−Mo_2 δ communication is minimized. Recently fulvanato-bridged Mo_4 species were fully characterized in their neutral and oxidized forms.[40] Here the N_2CCN_2 bridge is planar being contained within two fused six-membered rings and is thus stereochemically and isolobally related to the oxalate bridge. The mixed valence compound was shown to be class III by both crystallography and the appearance of its charge resonance band in the near-IR, which by both shape and energy was similar to that shown in Figure 8 for the oxalate-bridged Mo_4 cation.

An interesting comparison of the coupling between Mo_4- and W_4-containing complexes is seen for 3,6-dioxypyridazine complexes (**C**).[17,23] As noted earlier, this bridge aligns the metal atoms such that inner atoms, those bonded to the nitrogens are only 3.3 Å apart. The electrochemical data (Table 1), EPR spectra, and absorption data (Table 2) indicate that the radical cations are fully delocalized, class III. It is, however, also apparent that in comparison to the oxalate bridge the electronic coupling is weaker for the tungsten complex but slightly enhanced for molybdenum. Again this can be understood in terms of the M_2 δ orbital interactions with the bridge π-system. The W_2 δ orbitals lie closer in energy to the oxalate LUMO than the 3,6-dioxypyridazine bridge LUMO. However, the nitrogen pπ orbital is higher in energy in relation to the oxygen pπ, so for molybdenum, whose Mo_2 δ orbital is ca. 0.5 eV lower in energy than that of the tungsten analogue, there is a greater mixing of the bridge π orbital in the HOMO. Thus in the spin exchange model, hole transfer may also contribute to the coupling. However, it is still evident that the coupling is greater for the tungsten complex, which confirms that the dominant mechanism of coupling is via electron transfer through the bridge.

Concluding Remarks

The occurrence of M_2 δ-to-bridge π conjugation in these dicarboxylate and closely related bridged [M_2−bridge−M_2] compounds leads to a number of interesting physical properties including thermo-, solvato-, and electrochromic behavior. In their singly oxidized forms, the complexes are seen to traverse the classifications of mixed valence compounds from valence trapped, class II, and fully delocalized, class III. The attendant rich spectroscopic data coupled with electronic structure calculations clearly identify the origin of electronic coupling as electron transfer via the bridge. Even when the orbital energy of bridge-based π-orbitals are close in energy to the metal δ orbitals, hole transfer does not take over because the CO_2 unit acts as a gate. Substituting oxygen by sulfur or a NR group within the CO_2 unit can enhance the electronic coupling as a result of greater mixing with the metal δ orbitals. Electron delocalization in the W_4-containing mixed valence ions to nearly 14 Å places some of these ions as rare examples of class III behavior beyond 10 Å. The ability to control the degree of electronic coupling through the bridge by physical and chemical reactions affords the potential development of molecular signaling and switching, and this notion is being pursued.

We thank our talented co-workers and collaborators listed in the references. We also thank the National Science Foundation for financial support of this work and the Ohio Super Computing Center for generous allocation of computing resources.

References

(1) Robin, M. B.; Day, P. Mixed valence chemistry. A survey and classification. *Adv. Inorg. Radiochem.* **1967**, *10*, 247−422.
(2) Hush, N. S. Intervalence-transfer absorption. II. Theoretical considerations and spectroscopic data. *Prog. Inorg. Chem.* **1967**, *8*, 391−444.
(3) Creutz, C.; Taube, H. Direct approach to measuring the Franck−Condon barrier to electron transfer between metal ions. *J. Am. Chem. Soc.* **1969**, *91*, 3988−3989.
(4) Cowan, D. O.; LeVanda, C.; Park, J.; Kaufman, F. Organic solid state. VIII. Mixed-valence ferrocene chemistry. *Acc. Chem. Res.* **1973**, *6*, 1−7.
(5) Creutz, C. Mixed valence complexes of d^5-d^6 metal centers. *Prog. Inorg. Chem.* **1983**, *30*, 1−73.
(6) Ward, M. D. Metal-metal interactions in binuclear complexes exhibiting mixed valency; molecular wires and switches. *Chem. Soc. Rev.* **1995**, *24*, 121−134.
(7) Clark, R. J. H. Tilden Lecture. The chemistry and spectroscopy of mixed-valence complexes. *Chem. Soc. Rev.* **1984**, *13*, 219−244.
(8) Nelsen, S. F. "Almost delocalized" intervalence compounds. *Chem.—Eur. J.* **2000**, *6*, 581−588.
(9) Brunschwig, B. S.; Creutz, C.; Sutin, N. Optical transitions of symmetrical mixed-valence systems in the Class II−III transition regime. *Chem. Soc. Rev.* **2002**, *31*, 168−184.
(10) Piepho, S. B. Vibronic coupling model for the calculation of mixed-valence line shapes: a new look at the Creutz-Taube ion. *J. Am. Chem. Soc.* **1990**, *112*, 4197−4206.
(11) Hupp, J. T.; Williams, R. D. Using resonance Raman spectroscopy to examine vibrational barriers to electron transfer and electronic delocalization. *Acc. Chem. Res.* **2001**, *34*, 808−817.
(12) Ito, T.; Imai, N.; Yamaguchi, T.; Hamaguchi, T.; Londergan, C. H.; Kubiak, C. P. Observation and dynamics of "Charge-Transfer Isomers". *Angew. Chem., Int. Ed.* **2004**, *43*, 1376−1381.
(13) Salsman, J. C.; Kubiak, C. P.; Ito, T. Mixed valence isomers. *J. Am. Chem. Soc.* **2005**, *127*, 2382−2383.

(14) Demadis, K. D.; Hartshorn, C. M.; Meyer, T. J. The localized-to-delocalized transition in mixed-valence chemistry. *Chem. Rev.* **2001**, *101*, 2655−2686.
(15) Cotton, F. A.; Murillo, C. A.; Walton, R. A. *Multiple Bonds between Metal Atoms*, 3rd ed.; Springer Science and Business Media, Inc.: New York, 2005.
(16) Cotton, F. A.; Dalal, N. S.; Liu, C. Y.; Murillo, C. A.; North, J. M.; Wang, X. Fully localized mixed-valence oxidation products of molecules containing two linked dimolybdenum units: An effective structural criterion. *J. Am. Chem. Soc.* **2003**, *125*, 12945−12952.
(17) Chisholm, M. H.; Clark, R. J. H.; Gallucci, J. C.; Hadad, C. M.; Patmore, N. J. Electronically-coupled tungsten-tungsten quadruple bonds: Comparisons of electron delocalization in 3,6-dioxypyridazine and oxalate-bridged compounds. *J. Am. Chem. Soc.* **2004**, *126*, 8303−8313.
(18) Hopkins, M. D.; Gray, H. B.; Miskowski, V. M. $\delta \rightarrow \delta^*$ Revisited: What the energies and intensities mean. *Polyhedron* **1987**, *6*, 705−714.
(19) Clark, R. J. H.; Hempleman, A. J.; Kurmoo, M. Infrared, Raman, and resonance-Raman spectra of $[Mo_2(O_2CCH_3)_4]$ and $[Mo_2(O_2CCD_3)_4]$. *J. Chem. Soc., Dalton Trans.* **1988**, 973−981.
(20) Chisholm, M. H.; Pate, B. D.; Wilson, P. J.; Zaleski, J. M. On the electron delocalization in the radical cations formed by oxidation of MM quadruple bonds linked by oxalate and perfluoroterephthalate bridges. *Chem. Commun.* **2002**, 1084−1085.
(21) Chisholm, M. H.; D'Acchioli, J. S.; Pate, B. D.; Patmore, N. J.; Dalal, N. S.; Zipse, D. J. Cations $M_2(O_2C^tBu)_4^+$, where M = Mo and W, and $MoW(O_2C^tBu)_4^+$. Theoretical, spectroscopic, and structural investigations. *Inorg. Chem.* **2005**, *44*, 1061−1085.
(22) Cayton, R. H.; Chisholm, M. H.; Huffman, J. C.; Lobkovsky, E. B. Metal−metal multiple bonds in ordered assemblies. 1. Tetranuclear molybdenum and tungsten carboxylates involving covalently linked metal-metal quadruple bonds. Molecular models for subunits of one-dimensional stiff-chain polymers. *J. Am. Chem. Soc.* **1991**, *113*, 8709−8724.
(23) Cayton, R. H.; Chisholm, M. H.; Putilina, E. F.; Folting, K. Covalenty linked molybdenum−molybdenum quadruple bonds. Dioxypyridazine dianion and 2-imidazolinethionate as bridges between dimolybdenum fragments. *Polyhedron* **1993**, *12*, 2627−2633.
(24) Bursten, B. E.; Chisholm, M. H.; Clark, R. J. H.; Firth, S.; Hadad, C. M.; MacIntosh, A. M.; Wilson, P. J.; Woodward, P. M.; Zaleski, J. M. Oxalate-bridged complexes of dimolybdenum and ditungsten supported by pivalate ligands: $(^tBuCO_2)_3M_2(\mu\text{-}O_2CCO_2)\text{-}M_2(O_2C^tBu)_3$. Correlation of the solid-state, molecular, and electronic structures with Raman, resonance Raman, and electronic spectral data. *J. Am. Chem. Soc.* **2002**, *124*, 3050−3063.
(25) Byrnes, M. J.; Chisholm, M. H.; Clark, R. J. H.; Gallucci, J. C.; Hadad, C. M.; Patmore, N. J. Thienyl carboxylate ligands bound to and bridging MM quadruple bonds, M = Mo or W: Models for polythiophenes incorporating MM quadruple bonds. *Inorg. Chem.* **2004**, *43*, 6334−6344.
(26) Chisholm, M. H.; Chou, R. Manuscript in preparation.
(27) Chisholm, M. H.; Patmore, N. J. On the solvatochromic properties of the oxalate-bridged complexes $[(^tBuCO_2)_3M_2]_2(\mu\text{-}O_2C_2O_2)$ where M = Mo or W. *Inorg. Chim. Acta.* **2004**, *357*, 3877−3882.
(28) Richardson, D. E.; Taube, H. Determination of $E_2^\circ - E_1^\circ$ in multistep charge transfer by stationary-electrode pulse and cyclic voltammetry: Application to binuclear ruthenium ammines. *Inorg. Chem.* **1981**, *20*, 1278−1285.
(29) D'Alessandro, D. M.; Keene, F. R. A cautionary warning on the use of electrochemical measurements to calculate comproportionation constants for mixed-valence compounds. *Dalton Trans.* **2004**, 3950−3954.
(30) Barriere, F.; Camire, N.; Geiger, W. E.; Mueller-Westerhoff, U. T.; Sanders, R. Use of medium effects to tune the $\Delta E_{1/2}$ values of bimetallic and oligometallic compounds. *J. Am. Chem. Soc.* **2002**, *124*, 7262−7263.
(31) D'Acchioli, J. S. Ph.D. Thesis, The Ohio State University, Columbus, OH, 2005.
(32) Chisholm, M. H.; Feil, F.; Hadad, C. M.; Patmore, N. J. Electronically coupled MM quadruply-bonded complexes (M = Mo or W) employing functionalized terephthalate bridges: Toward molecular rheostats and switches. *J. Am. Chem. Soc.* **2005**, *127*, 18150−18158.
(33) Cayton, R. H.; Chisholm, M. H. Electronic coupling between covalently linked metal-metal quadruple bonds of molybdenum and tungsten. *J. Am. Chem. Soc.* **1989**, *111*, 8921−8923.
(34) Barybin, M. V.; Chisholm, M. H.; Dalal, N. S.; Holovics, T. H.; Patmore, N. J.; Robinson, R. E.; Zipse, D. J. Long-range electronic coupling of MM quadruple bonds (M = Mo or W) via a 2,6-azulenedicarboxylate bridge. *J. Am. Chem. Soc.* **2005**, *127*, 15182−15190.
(35) Chisholm, M. H.; Griffin, H.; Patmore, N. J. Manuscript in preparation.
(36) Chisholm, M. H.; D'Acchioli, J. S.; Hadad, C. M.; Patmore, N. J. Studies of oxalate-bridged MM quadruple bonds and their radical cations (M = Mo or W): On the matter of linkage isomers. *Dalton Trans.* **2005**, 1852−1857.
(37) Chisholm, M. H.; Patmore, N. J. Unpublished work.
(38) Chisholm, M. H.; Patmore, N. J. Electronic coupling in 1,4-$(COS)_2\text{-}C_6H_4$ Linked MM Quadruple Bonds (M = Mo, W): The influence of S for O substitution. *Dalton Trans.* **2006**, 3164−3169.
(39) Cotton, F. A.; Liu, C. Y.; Murillo, C. A.; Villagran, D.; Wang, X. Modifying electronic communication in dimolybdenum units by linkage isomers of bridged oxamidate dianions. *J. Am. Chem. Soc.* **2003**, *125*, 13564−13575.
(40) Cotton, F. A.; Li, Z.; Liu, C. Y.; Murillo, C. A.; Villagran, D. Strong electronic interaction between two dimolybdenum units linked by a tetraazatetracene. *Inorg. Chem.* **2006**, *45*, 767−778.

AR068100I